

## Characterization of helium discharge cleaning plasmas in ADITYA tokamak using collisional-radiative model code

Ram Prakash, P. Vasu, Vinay Kumar, R. Manchanda, M. B. Chowdhuri, and M. Goto

Citation: [Journal of Applied Physics](#) **97**, 043301 (2005); doi: 10.1063/1.1847704

View online: <http://dx.doi.org/10.1063/1.1847704>

View Table of Contents: <http://scitation.aip.org/content/aip/journal/jap/97/4?ver=pdfcov>

Published by the [AIP Publishing](#)

---

### Articles you may be interested in

[Characteristics of microinstabilities in electron cyclotron and ohmic heated discharges](#)

Phys. Plasmas **18**, 082506 (2011); 10.1063/1.3620409

[Analysis of metallic impurity density profiles in low collisionality Joint European Torus H-mode and L-mode plasmas](#)

Phys. Plasmas **13**, 042501 (2006); 10.1063/1.2187424

[Active and fast particle driven Alfvén eigenmodes in Alcator C-Moda\)](#)

Phys. Plasmas **12**, 056102 (2005); 10.1063/1.1865012

[Relationship between density peaking, particle thermodiffusion, Ohmic confinement, and microinstabilities in ASDEX Upgrade L -mode plasmas](#)

Phys. Plasmas **12**, 040701 (2005); 10.1063/1.1867492

[Effects of high density peaking and high collisionality on the stabilization of the electrostatic turbulence in the Frascati Tokamak Upgrade](#)

Phys. Plasmas **11**, 3845 (2004); 10.1063/1.1766031

---



# Characterization of helium discharge cleaning plasmas in ADITYA tokamak using collisional-radiative model code

Ram Prakash, P. Vasu,<sup>a)</sup> Vinay Kumar, R. Manchanda, and M. B. Chowdhuri  
*Institute for Plasma Research, Bhat, Gandhinagar-382428, Gujarat, India*

M. Goto  
*National Institute for Fusion Science, Toki 509-5292, Japan*

(Received 30 June 2004; accepted 16 November 2004; published online 20 January 2005)

The wall conditioning of the ADITYA tokamak is usually done, by first producing an electron cyclotron resonance (ECR) plasma inside the vessel and then superimposing a pulsed ohmic discharge on the ECR background. Sometimes, helium gas is used as a working gas. In this article, the spectral line emissions of neutral helium for the two different plasmas—namely, the ECR and the pulsed discharge cleaning (PDC) plasmas—have been analyzed using a collisional-radiative (CR)-model code to estimate the electron density and temperature. We are able to match the experimentally obtained relative intensity ratios with those predicted by the model under the assumption of ionizing plasma condition if the possible effects of the metastable states are not ignored. This has been done by using the populations of two metastable levels ( $2^1S$  and  $2^3S$ ) as independent parameters in addition to the ground states of neutrals and ions in the CR model under a quasisteady-state approximation. It is further seen that, it is the metastables and not the recombination (including dielectronic) processes that lead to a better fit with experimental observations. The column density of neutrals inferred from this analysis implies that the emission from the PDC discharge emanates from a large region of the vessel, while in the ECR discharge, the plasma responsible for the emission is restricted to a narrow region. This is also borne out by experimental observation. © 2005 American Institute of Physics. [DOI: 10.1063/1.1847704]

## I. INTRODUCTION

In the fusion plasma, the nonhydrogenic atoms and ions of commonly occurring impurity elements are of concern because they contribute significantly to the plasma radiation losses and adversely affect the plasma performance. The control of both hydrogen and impurity atoms is important for obtaining reproducible tokamak discharges. This is usually achieved by wall conditioning/cleaning, i.e., removal of adsorption from plasma facing surfaces. The principal methods for conditioning the graphite tiles for plasma discharge operation in tokamaks are baking, He-glow discharge cleaning, boronization, carbonization, and lithiumization, etc.<sup>1</sup> The common methods of wall cleaning are glow discharge cleaning (GDC), Taylor discharge cleaning (TDC), vacuum baking, and electron cyclotron resonance-discharge cleaning (ECR-DC), etc.<sup>2</sup> These methods are effective in specific cleaning/conditioning depending on the gas used and the operational range of plasma parameters. Thus, it becomes relevant to characterize the discharge used for cleaning/conditioning to optimize the process and spectroscopic observations on the plasma offer a means to do so.

The relative intensities of spectral lines emitted from different upper levels are obviously proportional to the relative populations of these levels, which in turn depend on the plasma parameters (i.e.,  $N_e$  and  $T_e$ ). Using the collisional-radiative (CR) model<sup>3–5</sup> it is possible to calculate the expected relative intensities of various lines of specie for a

given value of  $N_e$  and  $T_e$ . Such calculations can be done at various degrees of sophistication by including as many atomic processes (i.e., processes of populating or depopulating various levels) as are judged to be relevant. When more processes are included, the prediction can be more reliable but at a greater computational effort. Considerable advances have been made in the last few decades in the calculation of accurate cross sections necessary for the rate coefficients, and many codes based on the CR model, for example, the ADAS,<sup>5</sup> ALADDIN,<sup>6,7</sup> and CHIANTI,<sup>8</sup> etc., have been developed. For neutral helium line emissions from fusion plasmas, a complete CR-model code along with the relevant database has been developed.<sup>4,9</sup>

Using the above code, Kubo *et al.*<sup>10</sup> have characterized the JT-60U divertor plasma from the neutral helium line emissions and the obtained results are found to be in good agreement with the Langmuir probe measurements. These results are interpreted under the assumptions that the plasma is purely ionizing and that quasisteady-state approximation is valid for all the levels, except ground-state atoms and ions. This treatment is adequate for the investigations of divertor plasma because of the high electron plasma densities ( $N_e > 10^{12}$  cm<sup>-3</sup>). However, at lower plasma densities the metastable state populations can affect the excited-state population considerably<sup>11</sup> due to the long relaxation times of these levels (e.g.,  $2^3S \sim 0.1$  ms) in the absence of frequent collisions. Furthermore, the electron collisional excitation rates of metastable level may exceed the excitation rates from the ground-state atoms by orders of magnitude.<sup>12</sup>

In the present work, we have used the above CR code for

<sup>a)</sup>Electronic mail: vasu@ipr.res.in

helium<sup>9</sup> for interpreting the spectra from the cleaning discharges of the ADITYA tokamak. The experimental procedure is summarized in Sec. II. A preliminary analysis of our experimental results was made by comparing with computed results obtained<sup>13</sup> for ionizing plasma under the validity condition of quasisteady-state approximation for the two metastable states apart from the excited states. In Sec. III A, we describe this analysis. This analysis yielded, for two types of discharges, namely, the electron cyclotron resonance (ECR) and the pulsed discharge cleaning (PDC) plasmas, temperatures larger than 20 eV and electron densities lower than  $10^{12} \text{ cm}^{-3}$ . This makes one suspect that the assumptions made in this analysis may not be appropriate because at lower densities ( $N_e < 10^{12} \text{ cm}^{-3}$ ) the metastable state population could be significant and at higher temperatures the dielectronic recombinations may be appreciable and the consideration of these processes can affect the excited-state populations considerably.

To understand these effects clearly, in this work, a more detailed investigation of the data has been performed. The investigations are carried out for ionizing plasma, both when the metastables are also included in the quasisteady-state approximation and when they are excluded. The effects of recombinations (including dielectronic recombination) have also been examined. It turned out that at lower densities the effects of metastables are more important than the recombinations. Exclusion of the metastables from the quasisteady-state assumption in the CR model leads to a better match to our observations. These are described in Secs. III B and III C. The results are summarized and discussed in Sec. IV.

## II. EXPERIMENT

In ADITYA tokamak,<sup>14</sup> the ECR and pulsed discharge plasma of hydrogen/helium gas are often used for the cleaning purposes before going on to any regular discharge. Consequently, there is an ongoing interest in characterizing such plasmas for improving our cleaning operation. The helium atom is an attractive diagnostic specie for electron temperature and density measurements spectroscopically. It has various advantages, for example, well-known atomic data, strong visible lines, and availability of many density or temperature sensitive line pairs for diagnostics.<sup>13</sup>

The experiments are carried out in the vacuum vessel of ADITYA tokamak with a major radius of 75 cm and a minor radius of 25 cm. In ADITYA, the usual cleaning procedure is a pulsed ohmic discharge superimposed on a continuous ECR plasma. A toroidal magnetic field of  $B_T \sim 0.05 \text{ T}$  and a gas pressure of  $\sim 2.5 \times 10^{-5} \text{ Torr}$  is used. The ECR plasma is produced using a magnetron ECR source with a frequency of  $\sim 2.45 \text{ GHz}$ . On the ECR background, the pulsed discharge cleaning (PDC) plasma is produced (lasting about 5 ms) once every  $\sim 4 \text{ s}$ . For spectroscopic studies, the light emitted during the discharges is relayed by optical fibers and fed to the visible monochromator fitted with an intensified charge-coupled device (CCD) camera-based acquisition system to record the emission lines. To capture the plasma emissions during the 5-ms window, when both the ECR and the PDC are on (i.e., ECR+PDC), the loop voltage is used to trigger

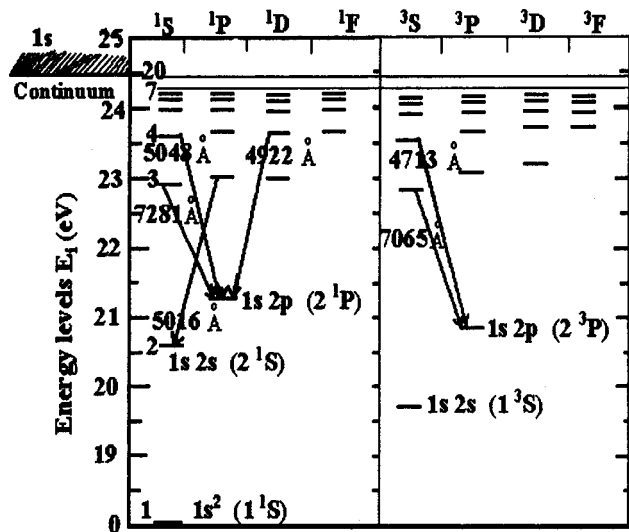


FIG. 1. Partial Grotrian diagram of the helium atom.

the acquisition system. An exposure time of 5 ms was found satisfactory. For recording the spectrum of ECR plasma alone, the acquisition is triggered after a 10-ms delay and an exposure of 70 ms was used.

The experimental spectra have been recorded with a resolution of  $\sim 2.5 \text{ \AA}$ . This was adequate to observe well-isolated He I lines such as 4713, 4922, 5016, 5048, 7065, and 7281  $\text{\AA}$ , yielding sufficient signal strength for quantitative analysis. The transitions of these lines are shown in the energy-level diagram (see Fig. 1). The experimental values of line intensity ratio of  $I(4922 \text{ \AA})/I(5048 \text{ \AA})$ ,  $I(7281 \text{ \AA})/I(7065 \text{ \AA})$ ,  $I(5048 \text{ \AA})/I(4713 \text{ \AA})$ , and  $I(5016 \text{ \AA})/I(4713 \text{ \AA})$  comes out to be 3.12, 0.23, 0.3, and 2.17, respectively, for the (ECR+PDC) discharge after correcting for the wavelength-dependent detection system separately. For the ECR alone, the values of these ratios are typically 1.39, 0.7, 0.67, and 3.92, respectively. The statistical uncertainty (i.e., trial-to-trial variation) is about  $\pm 5\%$  of the observed ratios.

## III. COLLISIONAL-RADIATIVE MODEL AND DATA ANALYSIS

### A. Analysis under the validity condition of quasisteady-state approximation for the two metastable states

Intensities of the He I lines are calculated using the CR-model code for helium.<sup>9</sup> The atomic physics database needed is a part of the code itself and has been in wide use. We have used this data without any further evaluation.

Under the assumption that the dominant populations are ground-state atoms and ions and the quasisteady-state approximation is valid for the populations of all excited levels including metastable states, the population  $N_u$  of an excited level  $u$  is expressed as

$$N_u = R_0(u)N_eN_i + R_I(u)N_eN_g, \quad (1)$$

where  $R_0(u)$  and  $R_I(u)$  are the reduced population coefficients for the level  $u$ . Here  $N_i$ ,  $N_g$ , and  $N_e$  represent ground-state helium ion, ground-state helium atom, and electron

densities, respectively. The rate equations for independent levels are

$$\frac{dN_g}{dt} = -\frac{dN_i}{dt} = \alpha_{CR}N_iN_e - S_{CR}N_gN_e, \quad (2)$$

where  $\alpha_{CR}$  and  $S_{CR}$  are the collisional-radiative recombination and ionization rate coefficients, respectively. The reduced population coefficients and the collisions-radiative rate coefficients are functions of  $N_e$  and  $T_e$  only and are calculated from the code by considering all the processes of populating and depopulating the level  $u$  by excitation, deexcitation, spontaneous emission, ionization, and recombination from the adjacent ionization states, etc.<sup>9</sup>

In Eq. (1), the population that is proportional to the helium ion density is the recombination component, and proportional to the helium atom density is the ionizing component. Under ionizing condition the term  $R_0(u)N_eN_i$  is taken to be negligibly small<sup>12</sup> and the line intensity  $I_{ul}$  for a transition from level  $u$  to level  $l$  is expressed as

$$I_{ul} = \frac{1}{4\pi}N_uA_{ul}\Delta x$$

$$= \frac{1}{4\pi}R_1(u)A_{ul}N_gN_e\Delta x \quad \text{photons cm}^{-3} \text{ s}^{-1} \text{ sr}^{-1} \quad (3)$$

$$= \frac{1}{4\pi}X_{ul}N_gN_e\Delta x, \quad (4)$$

where  $A_{ul}$  is the transition probability for the level  $l$ ,  $\Delta x$  is the length of the observed plasma column, and  $X_{ul}$  is an emission rate coefficient that depends on  $N_e$  and  $T_e$  only. The significance of the emission rate coefficient is that the experimentally observable intensity ratio of two lines (which is not directly dependent on  $N_i$ ,  $N_g$ , and  $N_e$ ) can be easily obtained from the code as the ratio of corresponding emission rate coefficients (i.e.,  $I_{ul}/I_{u'l'} = X_{ul}/X_{u'l'}$ ). Thus, it is easy to calculate the expected ratio of two lines under different plasma conditions of  $N_e$  and  $T_e$ .

The intensity ratios  $I(4922 \text{ \AA})/I(5048 \text{ \AA})$ ,  $I(7281 \text{ \AA})/I(7065 \text{ \AA})$ ,  $I(5048 \text{ \AA})/I(4713 \text{ \AA})$ , and  $I(5016 \text{ \AA})/I(4713 \text{ \AA})$  are shown in Fig. 2. The ratios  $I(7281 \text{ \AA})/I(7065 \text{ \AA})$  and  $I(5048 \text{ \AA})/I(4713 \text{ \AA})$  depend more on temperature and weakly on the density, and ratio  $I(4922 \text{ \AA})/I(5048 \text{ \AA})$  depends more on the density and weakly on the temperature.<sup>13</sup> A comparison of our observed ratio with the calculated ratio of  $I(4922 \text{ \AA})/I(5048 \text{ \AA})$  reveals the electron density in the range of  $(6 \pm 1) \times 10^{11} \text{ cm}^{-3}$  for the ECR+PDC plasma and  $(5 \pm 5) \times 10^{10} \text{ cm}^{-3}$  for the ECR plasma. The temperature is estimated from  $I(5048 \text{ \AA})/I(4713 \text{ \AA})$  and is found to be  $(25 \pm 5) \text{ eV}$  for the ECR+PDC plasma and  $(60 \pm 5) \text{ eV}$  for the ECR plasma alone. The observed ratio of  $I(7281 \text{ \AA})/I(7065 \text{ \AA})$  does not match the calculated values for similar values of  $N_e$  and  $T_e$ . Also, the ratio  $I(5016 \text{ \AA})/I(4713 \text{ \AA})$  does not even fall in the range of the corresponding ratio obtained from the code. So, when we are using more than two ratios, the above analysis shows that for the ionizing plasma under the validity condition of the

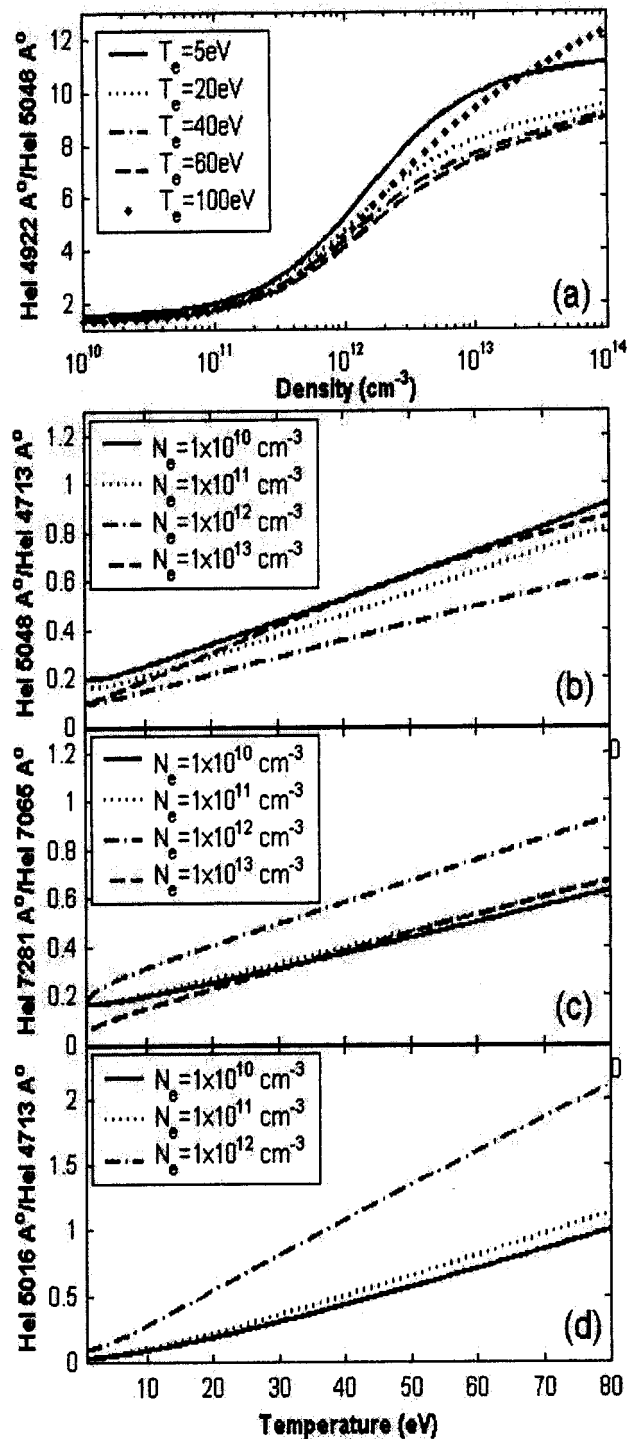


FIG. 2. Calculated line intensity ratios at different  $N_e$  and  $T_e$  for the ionizing plasma under the validity condition of quasisteady-state approximation for the two metastable states. (a)  $I(4922 \text{ \AA})/I(5048 \text{ \AA})$ , (b)  $I(5048 \text{ \AA})/I(4713 \text{ \AA})$ , (c)  $I(7281 \text{ \AA})/I(7065 \text{ \AA})$ , and (d)  $I(5016 \text{ \AA})/I(4713 \text{ \AA})$ .

quasisteady-state approximation for the metastable states, the estimated values of  $N_e$  and  $T_e$  are poorly determined. As a measure of mismatch, we use the variance

$$\sigma(T_e, N_e) = \sqrt{\frac{1}{4} \sum_{i=1}^4 \left\{ \frac{R_i(x) - R_i(c)}{R_i(x)} \right\}^2}, \quad (5)$$

where  $R_i(x)$  represents the experimental ratios and  $R_i(c)$  represents the corresponding calculated ratios from the code.



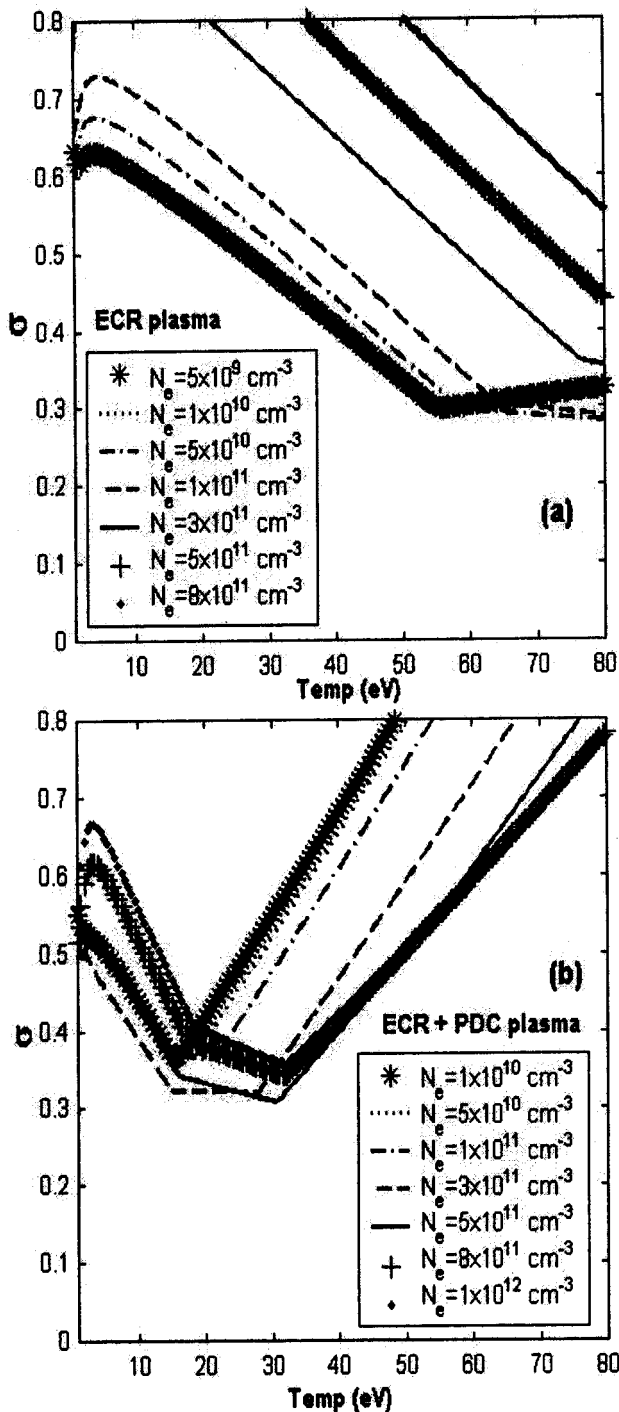


FIG. 3. Variance ( $\sigma$ ) at different  $N_e$  and  $T_e$  for the ionizing plasma under the validity condition of quasisteady-state approximation for the two metastable states. (a) ECR plasma, and (b) ECR+PDC plasma.

The index “ $i$ ” is summed over all the used ratios, and in the present case, it is four.

The variance at different temperatures and densities about the expected values is shown in Fig. 3. For the ECR+PDC the best fit has  $\sigma \sim 0.31$  and for the ECR  $\sigma \sim 0.29$ . The rather high value of inferred temperature (i.e.,  $\sim 55$  eV for the ECR plasma) and the low densities (i.e.,  $< 10^{12}$   $\text{cm}^{-3}$  for both the cases), leads us to probe if a better match could be obtained when either dielectronic recombination or metastable effects are also accounted for. It is to be noted that the

poor match is mainly on account of the two ratios  $I(5016 \text{ \AA})/I(4713 \text{ \AA})$  and  $I(7281 \text{ \AA})/I(7065 \text{ \AA})$ , both of which include triplet transitions. This suggests a possible role of the  $2^3S$  metastable state in determining the upper state populations because a triplet-to-triplet transition is more likely in the population process.<sup>15</sup> The quasisteady-state approximation may be overestimating the population of metastables, especially  $2^3S$  state.

## B. Effect of recombinations

First we considered the effect of recombinations assuming a purely recombining plasma (including dielectronic recombinations) in the original formulation to calculate the emission coefficients. Figure 4 shows the obtained ratios. It is seen that the obtained line ratios are very different from the observed ratios. Moreover, for realistic effect one should include both ionizing and recombining terms simultaneously and for this we need an estimation of  $N_i/N_g$ . Assuming this ratio to be the collisional-radiative quasisteady-state value (i.e.,  $N_i/N_g = S_{CR}/\alpha_{CR}$ ), we again calculated the line ratios for different  $N_e$  and  $T_e$ , which still could not be made to match the observed ratios. This analysis shows that the recombinations are unlikely to be important in the plasmas under consideration.

## C. Effect of metastables

In the lower-density regime it is possible that the formulation, in which metastables are treated as dependent levels on the ground-state atoms and ions, is not accurate. Under such circumstances the previous assumption of the quasisteady-state approximation is not valid for metastables. So, when metastables are to be treated as independent populations, (i.e., the quasisteady-state approximation in the CR model is assumed to be valid for the populations of all the levels except the ground-state atom, ion, and two metastables levels) Eq. (1) gets modified to

$$N_u = r_0(u)N_eN_i + r_1(u)N_eN_g + r_2(u)N_eN_{M1} + r_3(u)N_eN_{M2}. \quad (6)$$

Here  $r_0(u)$ ,  $r_1(u)$ ,  $r_2(u)$ , and  $r_3(u)$  are the population coefficients corresponding to the ground-state ion, atom, first metastable (singlet  $2^1S$ ), and second metastable (triplet  $2^3S$ ), respectively.  $N_{M1}$  and  $N_{M2}$  represent the number density of the first and second metastables, respectively.

As before, under the ionizing plasma condition, the line intensity of an emission line can be written as

$$\begin{aligned} I_{ul} &= \frac{1}{4\pi} N_u A_{ul} \Delta x = \frac{1}{4\pi} r_1(u) A_{ul} N_g N_e \Delta x \\ &= \frac{1}{4\pi} X'_{ul} N_g N_e \Delta x, \end{aligned} \quad (7)$$

where  $X'_{ul} = r_1(u) A_{ul}$  is the emission rate coefficient. Basically, the explicit consideration of metastables modifies the value of population coefficient to  $r_1(u)$  instead of  $R_1(u)$  in Eq. (3). Apparently the excited level populations of some of the triplet levels such as  $3^3S$  and  $4^3S$  get modified substantially, as shown in the Fig. 5. The influence on the

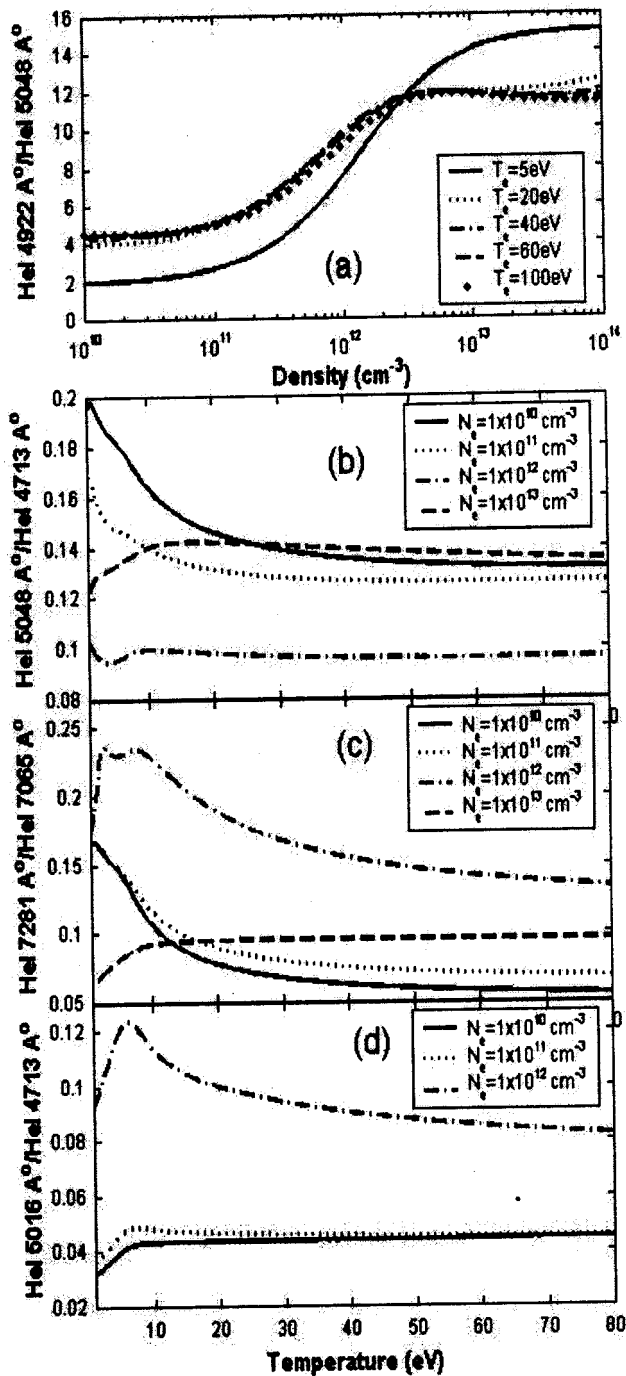


FIG. 4. Calculated line intensity ratios at different  $N_e$  and  $T_e$  for the recombining plasma. (a)  $I(4922 \text{ \AA})/I(5048 \text{ \AA})$ , (b)  $I(5048 \text{ \AA})/I(4713 \text{ \AA})$ , (c)  $I(7281 \text{ \AA})/I(7065 \text{ \AA})$ , and (d)  $I(5016 \text{ \AA})/I(4713 \text{ \AA})$ .

population of these levels is more at lower plasma densities (i.e., nearly an order of magnitude at  $N_e = 10^{10} \text{ cm}^{-3}$  for  $3^3S$  state). It is estimated that the contribution of the  $2^1S$  on the singlet lines is relatively small in comparison to that of the  $2^3S$  state on the triplet lines<sup>15</sup> (possibly due to the long relaxation time of the  $2^3S$  state in comparison to the  $2^1S$  state). This introduces a considerable modification in the interpretation of the line ratio measurements.

The line intensity ratios  $I(4922 \text{ \AA})/I(5048 \text{ \AA})$ ,  $I(7281 \text{ \AA})/I(7065 \text{ \AA})$ ,  $I(5048 \text{ \AA})/I(4713 \text{ \AA})$ , and  $I(5016 \text{ \AA})/I(4713 \text{ \AA})$  are calculated from the CR code for

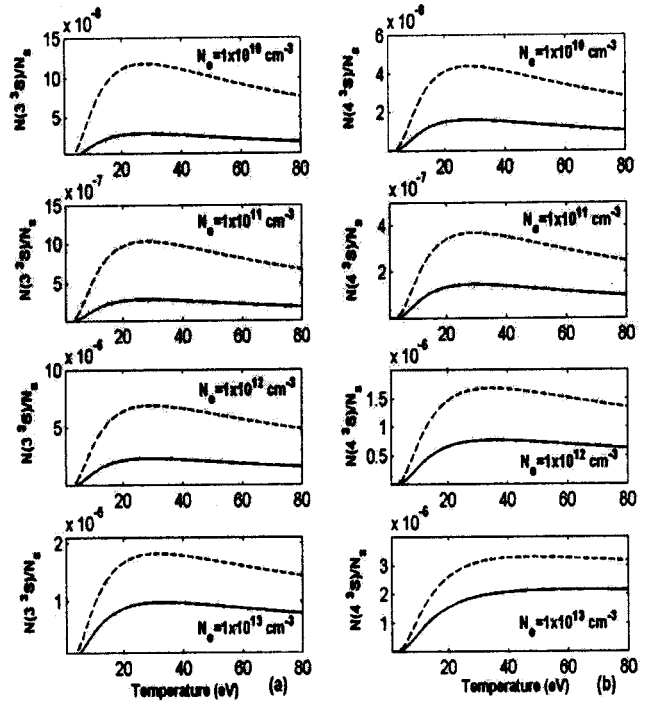


FIG. 5. Variation of the population densities of triplet excited levels (normalized by ground-state atom density) at different  $N_e$  and  $T_e$  for the ionizing plasma: two different cases, (dotted line) under the assumption of quasisteady-state approximation for the two metastable states, and (continuous line) when this assumption is relaxed. (a)  $1s3s (3^3S)$  state and (b)  $1s4s (4^3S)$  state.

ionizing plasma with metastables, and are shown in Fig. 6. The line ratio  $I(4922 \text{ \AA})/I(5048 \text{ \AA})$  again reflects density in the range of  $(7 \pm 2) \times 10^{11} \text{ cm}^{-3}$  for the ECR+PDC plasma and  $(5 \pm 5) \times 10^{10} \text{ cm}^{-3}$  for the ECR plasma alone. The ratios  $I(7281 \text{ \AA})/I(7065 \text{ \AA})$  and  $I(5048 \text{ \AA})/I(4713 \text{ \AA})$  produce temperatures of  $(7 \pm 2.5) \text{ eV}$  for the ECR+PDC plasma and  $(17 \pm 2.5) \text{ eV}$  for the ECR alone. Our observed ratio of  $I(5016 \text{ \AA})/I(4713 \text{ \AA})$  is also closer to the range of obtained ratio from the code, but still does not correspond to the  $N_e$  and  $T_e$  estimations made above. Sasaki *et al.*<sup>15</sup> have argued that the intensity of the 5016-Å line is affected by resonance scattering. This could be the reason of this disparity. We have also arrived at the best-fit values of  $N_e$  and  $T_e$  that match the experimental results using a minimum deviation, as shown in Fig. 7. The computed results fit the calculated results best with  $\sigma \sim 0.20$  at  $N_e \sim (9 \pm 1) \times 10^{11} \text{ cm}^{-3}$  and  $T_e \sim (8.5 \pm 1.5) \text{ eV}$  for the ECR+PDC discharge. For the ECR the best-fit value comes with  $\sigma \sim 0.24$  at  $N_e \sim (7.5 \pm 2.5) \times 10^{10} \text{ cm}^{-3}$  and  $T_e \sim (17 \pm 2.5) \text{ eV}$ . We see that accounting for metastables in ionizing plasma improves the  $N_e$  and  $T_e$  estimations, while the inclusion of recombinations did not.

We note here that, if the fractional abundances of metastables are known, a better fit to experimentally derived spectrum should be possible. Absorption techniques allow direct measurements of metastable populations especially at higher pressures. In many plasma experiments<sup>16-18</sup> this has been accomplished. The fact that only electron collisions can transfer atoms from the triplet to the singlet metastables has been utilized<sup>19</sup> to diagnose the plasma for both  $N_e$  and  $T_e$  by laser absorption techniques.

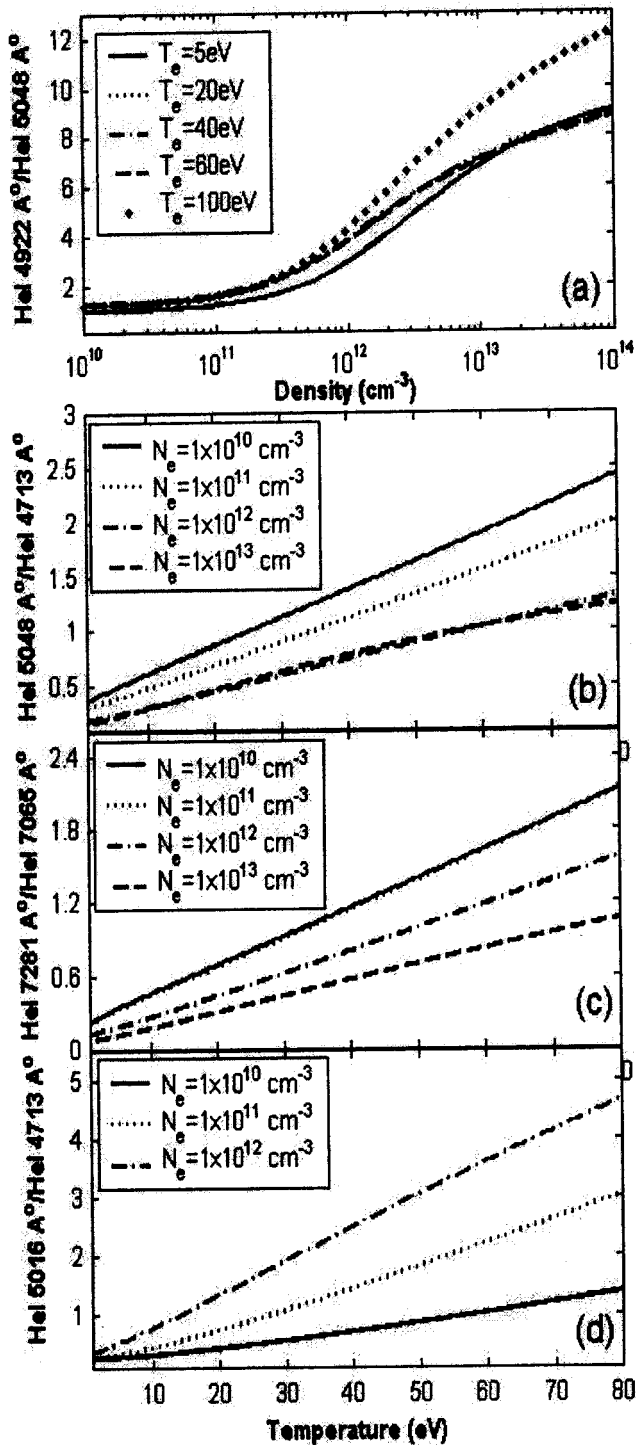


FIG. 6. Calculated line intensity ratios at different  $N_e$  and  $T_e$  for the ionizing plasma under the effects of metastables. (a)  $I(4922 \text{ \AA})/I(5048 \text{ \AA})$ , (b)  $I(5048 \text{ \AA})/I(4713 \text{ \AA})$ , (c)  $I(7281 \text{ \AA})/I(7065 \text{ \AA})$ , and (d)  $I(5016 \text{ \AA})/I(4713 \text{ \AA})$ .

#### IV. SUMMARY OF RESULTS AND DISCUSSIONS

The validity of the ionizing plasma condition is an important issue to be discussed. It is well known that the ionizing plasma condition holds well when  $N_i/N_g \ll S_{CR}/\alpha_{CR}$ .<sup>20</sup> To validate it, we need an estimation of  $N_i/N_g$ . If  $N_i$  is taken to be approximately equal to  $N_e$  (i.e., impurities and multiple ionization assumed negligible), from the filled gas pressure ( $\sim 1 \times 10^{12} \text{ cm}^{-3}$ ), it follows that in the ECR case  $N_g \approx 9$

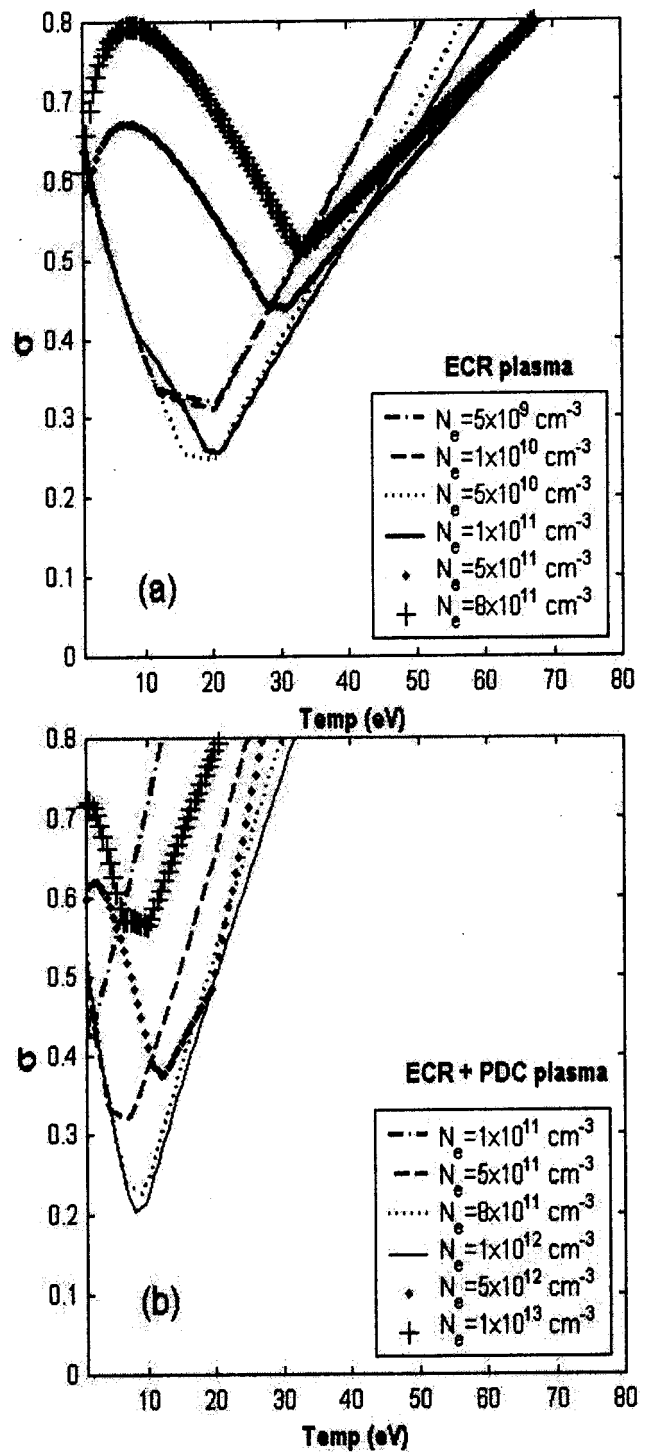
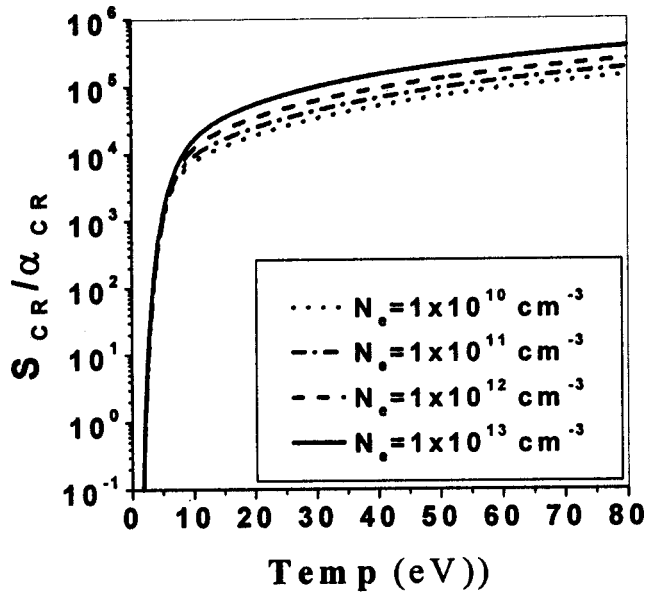


FIG. 7. Variance ( $\sigma$ ) at different  $N_e$  and  $T_e$  for the ionizing plasma under metastable effects. (a) ECR plasma and (b) ECR+PDC plasma.

$\times 10^{11} \text{ cm}^{-3}$  and  $(N_i/N_g)_{\text{ECR}} \sim 0.08$ . Similarly, the ECR +PDC plasma is 90% ionized and  $(N_i/N_g)_{\text{ECR+PDC}} \sim 9$ . From Fig. 8, where we have plotted the computed  $S_{CR}/\alpha_{CR}$  values, it is seen that for  $T_e > 3 \text{ eV}$  and  $N_e \sim 1 \times 10^{10} - 1 \times 10^{13} \text{ cm}^{-3}$  the required ionizing condition is easily satisfied and the assumption is valid for both of our plasma conditions.

Though the  $N_g$  has been estimated indirectly, we can calculate the column density ( $N_g \Delta x$ ) from the observed absolute intensities ( $I_{\text{obs}}$ ) and from Eq. (7) as

FIG. 8. Plot for the ratio  $S_{CR}/\alpha_{CR}$  at different  $N_e$  and  $T_e$ .

$$N_g \Delta x = \frac{4\pi I_{obs}}{(X'_{ul})_{eff} N_e} \quad (8)$$

Here  $\Delta x$  is the length of the emitting region of the plasma viewed by the optical system. The  $N_g \Delta x$  comes out to be  $\sim 1.62 \times 10^{11} \text{ cm}^{-2}$  for the ECR plasma (since the intensity of 5016-Å line may be affected by resonance scattering effect,<sup>15</sup> this line has not been used in this estimation). For the ECR+PDC plasma  $N_g \Delta x \sim 5.4 \times 10^{12} \text{ cm}^{-2}$ , which is about 33 times the ECR case, despite the lower neutral density. This implies that in the ECR plasma, the emitting region is much smaller than in the ECR+PDC plasma. A survey scan (with rather lower spatial resolution) across the vessel cross section, which is shown in Fig. 9, supports this inference. The ECR+PDC plasma emanates from the entire cross section while the ECR plasma emission region is confined to a narrow region.

In summary, we can say that the use of the CR-model code has enabled us to examine the roles of metastables and recombinations in spectra of plasmas of practical interest. It is seen that at the prevailing plasma densities ( $< 10^{12} \text{ cm}^{-3}$ ), the effects of metastable states of helium on the line intensities would be overestimated if the metastable states are assumed to be in a quasisteady-state (i.e., the population determined entirely by the ground-state populations).

We have shown that the computed values fit the observed results of the line ratio best at  $N_e \sim (9 \pm 1) \times 10^{11} \text{ cm}^{-3}$  and  $T_e \sim (8.5 \pm 1.5) \text{ eV}$  for the ECR+PDC discharge and  $N_e \sim (7.5 \pm 2.5) \times 10^{10} \text{ cm}^{-3}$  and  $T_e \sim (17 \pm 2.5) \text{ eV}$  for the ECR plasma. We have also verified that the ionizing plasma assumed for calculation holds good

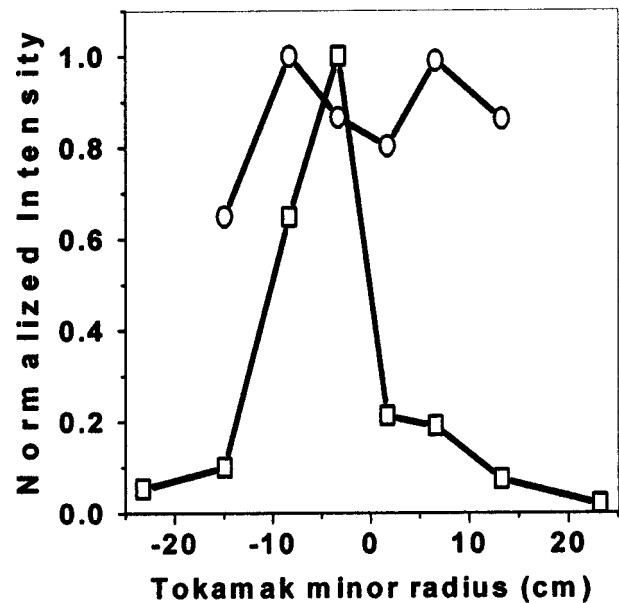


FIG. 9. Intensity variation of He I 7281 Å line (normalized by its peak value) vs tokamak minor radius: (□) for the ECR plasma, and (O) for the ECR+PDC plasmas.

for both, the ECR plasma that is restricted to a narrow region, and for the ECR+PDC plasma which nearly fills the entire vessel.

- <sup>1</sup>G. M. MaCracken and P. E. Stott, Nucl. Fusion **19**, 889 (1979).
- <sup>2</sup>R. Valencia, J. de la Rosa, E. Camps, G. Contreras, and S. Muhl, J. Nucl. Mater. **305**, 232 (2002).
- <sup>3</sup>D. R. Bates, A. E. Kingston, and R. W. P. McWhirter, Proc. R. Soc. London, Ser. A **257**, 297 (1962).
- <sup>4</sup>T. Fujimoto, J. Quant. Spectrosc. Radiat. Transf. **21**, 439 (1979).
- <sup>5</sup>H. P. Summers and M. von Hellermann, in "Atomic and Plasma-Material Interaction Processes in Controlled Thermonuclear Fusion," edited by R. K. Janev and H. W. Drawin (Elsevier, New York, 1993), p. 87.
- <sup>6</sup>R. A. Hulse, in "Atomic Processes in Plasmas," edited by Y. K. Kim and R. C. Elton, AIP Conf. Proc. No. 206 (AIP, New York, 1990), p. 63.
- <sup>7</sup>R. E. H. Clark and J. A. Stephens, in *The Atomic and Molecular Data Unit of the International Atomic Energy Agency*, edited by R. C. Mancini and R. A. Phaneuf, AIP Conf. Proc. No. 547 (AIP, New York, 2000), p. 167.
- <sup>8</sup>K. P. Dare, E. Landi, H. E. Mason, B. Monsignor Fossi, and P. R. Young, Astrophys. J., Suppl. Ser. **125**, 149 (1997).
- <sup>9</sup>M. Goto, J. Quant. Spectrosc. Radiat. Transf. **76**, 331 (2003).
- <sup>10</sup>H. Kubo, M. Goto, H. Takenaga, A. Kumagai, T. Sugie, S. Sakurai, N. Asakura, S. Higashijima, and A. Sakasai, J. Plasma Fusion Res. **75**, 954 (1999).
- <sup>11</sup>N. Brenning, J. Quant. Spectrosc. Radiat. Transf. **24**, 293 (1980).
- <sup>12</sup>Y. V. Ralchenko, R. K. Janev, T. Kato, D. V. Fursa, I. Bray, and F. J. de Heer, NIFS-DATA-59 (2000).
- <sup>13</sup>S. Sasaki, M. Goto, T. Kato, and S. Takamura, NIFS-DATA-49 (1998).
- <sup>14</sup>P. K. Atrey *et al.*, Indian J. Phys., B **66B**, 481 (1992).
- <sup>15</sup>S. Sasaki, S. Takamura, Shinichi Watanabe, S. Masuzaki, T. Kato, and K. Kadota, Rev. Sci. Instrum. **67**, 3521 (1996).
- <sup>16</sup>P. X. Feng, D. Andruczyk, B. W. James, K. Takiyama, S. Namba, and T. Oda, Plasma Sources Sci. Technol. **12**, 142 (2003).
- <sup>17</sup>D. Andruczyk, P. X. Feng, B. W. James, and J. Howard, Plasma Sources Sci. Technol. **11**, 426 (2002).
- <sup>18</sup>Tadahiro Kubota, Yoshihiko Morisaki, Atsushi Ohsawa, and Mikio Ohuchi, J. Phys. D **25**, 613 (1992).
- <sup>19</sup>E. A. Den Hartog, T. R. O'Brian, and J. E. Lawler, Phys. Rev. Lett. **62**, 1500 (1989).
- <sup>20</sup>T. Fujimoto and K. Sawada, NIFS-DATA-39 (1997).